CHEMISTRY OF MATERIALS
Article

Chem. Mater. **2009,** *21,* 2973–2979 2973
DOI:10.1021/cm900682q

Electronic Structure and Catalytic Study of Solid Solution of GaN in ZnO

Maitri Mapa,[†] K. S. Thushara,[†] Biswajit Saha,[‡] Purushottam Chakraborty,[‡] C. M. Janet,[§] R. P. Viswanath,[§] C. Madhavan Nair,[∥] K. V. G. K. Murty,[∥] and Chinnakonda S. Gopinath*,[†]

[†]*Catalysis Division, National Chemical Laboratory, Dr. Homi Bhabha Road, Pune 411 008, India,* [‡]*Surface Physics Division, Saha Institute of Nuclear Physics, 1/AF Bidhannagar, Kolkatta 700 064, India,* [§]*National Centre for Catalysis Research, Indian Institute of Technology − Madras, Chennai 600 036, India, and* [∥]*AU-KBC Research Center, MIT Campus of Anna University, Chromepet, Chennai 600 044, India*

Received March 10, 2009. Revised Manuscript Received April 17, 2009

Solid solutions of GaN in ZnO ($Zn_{1-z}Ga_z$)($O_{1-x}N_x$) (x and $z \leq 0.15$) have been prepared by simple solution combustion method. Except for minor changes in the lattice contraction, no significant change in the Wurtzite structure was observed. Raman and secondary ion mass spectrometry results show the direct Zn−N and Ga−N bonds in ($Zn_{1-z}Ga_z$)($O_{1-x}N_x$). Visible light absorption and XPS results demonstrate that N 2p states of nitride occupy the states above the O 2p valence band, and hence a change in optical band gap reduction occurs to ∼2.5 eV from 3.37 eV for ZnO. Significant nitrogen fixation catalytic activity through NH_3 formation has been observed at ambient pressure on virgin ($Zn_{1-z}Ga_z$)($O_{1-x}N_x$) material, indicating its potential as a catalyst.

1. Introduction

Band gap engineering of electronic materials is taking center stage as it is giving a new life to the known materials to use with desired and/or refined properties. ZnO is such a material and used in applications ranging from optoelectronics, gas sensing, and catalysis to cosmetics.[1−3] Doping in the ZnO lattice helps to reach many of the above applications. N-doping in ZnO was explored significantly, due to its compatible size to oxygen and nitrogen, has the smallest ionization energy.[1−3] Nitrogen doped ZnO (N-ZnO) was expected to create acceptors close to the valence band (VB) as a result of p-type doping. However, it leads to (a) p-type conductivity in N-ZnO,[2] which is not able to be reproduced by other groups even when the experimental conditions are the same,[3] and (b) deep acceptor levels that cannot induce p-type doping.[1,3,4] The above controversial results are due to poor reproducibility and low resistivity p-type ZnO.[1] N-ZnO films have been prepared by many sophisticated methods for optoelectronics applications, and there is no breakthrough yet.[1] Further, formation of Zn−O is energetically more favorable than Zn−N bonds, and a maximum of 3% N-doping in ZnO is reported to date, which is mainly due to poor solubility of nitrogen in ZnO.[1−3] However, our recent study demonstrated that a large amount of nitrogen could be introduced in the ZnO lattice by the solution combustion method, and N 2p states occupy midgap states without any change in bandgap.[4] Nevertheless, oxygen vacancy in ZnO, considered as a problem, was effectively utilized to introduce a large amount of nitrogen in ZnO. On the basis of the lattice energy analysis by codoping, two atom pairs (N−Ga or N−Al) were suggested to be effective for p-type doping in ZnO.[5] Ga^{3+} (0.62 Å) was preferred because its radii is close to Zn^{2+} (0.72 Å) and because

*To whom correspondence should be addressed: Ph: 0091-20-2590 2043. Fax: 0091-20-2590 2633. E-mail: cs.gopinath@ncl.res.in. Website: www.ncl.org.in/csgopinath.

(1) (a) Klingshrin, C. *Chem. Phys. Chem.* **2007**, *8*, 782. (b) Özgur, U.; Alivov, Y. I.; Liu, C.; Teke, A.; Reshchikov, M. A.; Dogan, S.; Avrutin, V.; Cho, S. J.; Morkoc, H. *J. Appl. Phys.* **2005**, *98*, 041301. (c) Karpina, V. A.; Lazorenko, V. I.; Lashkarev, C. V.; Dobrowolski, V. D.; Kopylova, L. I.; Baturin, V. A.; Pustovoytov, S. A.; Ju Karpenko, A.; Eremin, S. A.; Lytvyn, P. M.; Ovsyannikov, V. P.; Mazurenko, E. A. *Cryst. Res. Technol.* **2004**, *39*, 980. (d) Look, D. C.; Claflin, B. *Phys. Status Solidi B* **2004**, *241*, 624. (e) Velu, S.; Suzuki, K.; Gopinath, C. S. *J. Phys. Chem. B* **2002**, *106*, 12737. (f) Velu, S.; Suzuki, K.; Vijayaraj, M.; Gopinath, C. S. *Appl. Catal., B* **2005**, *55*, 287. (g) Velu, S.; Satoh, N.; Gopinath, C. S.; Suzuki, K. *Catal. Lett.* **2002**, *82*, 145. (h) Vijayaraj, M.; Gopinath, C. S. *J. Catal.* **2006**, *241*, 83.

(2) (a) Joseph, M.; Tabata, H.; Kawai, T *Jpn. J. Appl. Phys.* **1999**, *38*, L1205. (b) Look, D. C.; Reynolds, D. C.; Litton, C. W.; Jones, R. L.; Eason, D. B.; Cantwell, G *Appl. Phys. Lett.* **2002**, *81*, 1830. (c) Xiong, G.; Wilkinson, J.; Mischuck, B.; Tuzemen, S.; Ucer, K. B.; Williams, R. T. *Appl. Phys. Lett.* **2002**, *80*, 1195. (d) Perkins, C. L.; Lee, S. H.; Li, X.; Asher, S. E.; Coutts, T. J *J. Appl. Phys.* **2005**, *97*, 034907.

(3) (a) Iwata, K.; Fons, P.; Yamada, A.; Matsubara, K.; Niki, S *J. Cryst. Growth.* **2000**, *209*, 526. (b) Guo, X.-L.; Tabata, H.; Kawai, T *J. Cryst. Growth.* **2002**, *237*, 544. (c) Yamauchi, S.; Goto, Y.; Hariu, T *J. Cryst. Growth.* **2004**, *260*, 1.

(4) (a) Mapa, M.; Gopinath, C. S. *Chem. Mater.* **2009**, *21*, 351. (b) Murugan, B.; Srinivas, D.; Gopinath, C. S.; Ramaswamy, V.; Ramaswamy, A. V. *Chem. Mater.* **2005**, *17*, 3983. (c) Sathish, M.; Viswanathan, B.; Viswanath, R. P.; Gopinath, C. S. *Chem. Mater.* **2005**, *17*, 6349. (d) Gopinath, C. S. *J. Phys. Chem. B* **2006**, *110*, 7079. (e) Sathish, M.; Viswanath, R. P.; Gopinath, C. S. *J. Nanosci. Nanotechnol.* **2009**, *9*, 423.

(5) (a) Yamamoto, T.; Katayama-Yoshida, H *Jpn. J. Appl. Phys., Part 2* **1999**, *38*, L166. (b) Yamamoto, T.; Yoshida, H. K. *Physica B* **2001**, *302−303*, 155. (c) Yamamoto, T. *Thin Solid Films* **2002**, *420−421*, 100. (d) Singh, A. V.; Mehra, R. M.; Wakahara, A.; Yoshida, A. *J. Appl. Phys.* **2003**, *93*, 396. (e) Ohshima, T.; Ikegami, T.; Edihara, K; Asmussen, J.; Thareja, R. *Thin Solid Films* **2003**, *435*, 49.

Published on Web 05/21/2009

the Ga−N bond length (1.95 Å) is the same as that of Zn−O (1.97 Å), and it reduces the elastic contribution to the energy of the N-acceptor at O-sites.[5] It might minimize the deformation of the ZnO lattice even with high GaN content, since both exhibit Wurtzite structure. Formation of −N−Ga−N−Ga−N− clusters that occupy near-neighbor sites is favorable due to the strong attractive interaction between them, and it helps to increase the solubility of N in ZnO.[5] However, solid solution of a large amount of GaN in ZnO is not reported to date, which could be helpful for various applications from optoelectronics to catalysis. In the present study, up to 15 atom % nitrogen was introduced with up to 15 atom % Ga into ZnO, to prepare solid solution of GaN in ZnO or multifunctional $(Zn_{1-z}Ga_z)(O_{1-x}N_x)$. This material exhibits an electronic structure that is markedly different from ZnO and/or GaN. Being a good catalyst and/or support material, ZnO deserves to be explored for catalysis applications, especially when the electronic structure is significantly modified as in the above solid solution. These materials have been characterized by various methods, and N_2-fixation was explored via heterogeneous catalysis.

2. Experimental Section

2.1. Preparation of Catalysts. $Zn(NO_3)_2 \cdot 6H_2O$ (Merck), 0.1 M $Ga(NO_3)_3$ solution (Ga-metal (Aldrich) dissolved in HNO_3), and urea (Merck) were AR grade chemicals and used as such. Required metal nitrates and urea were taken in a 250 mL beaker with 10 mL of distilled water, stirred well, and then inserted into a furnace maintained at 500 °C. Water evaporates in 2−3 min followed by ignition of reactant mixture for the next 30 s yielding $(Zn_{1-z}Ga_z)(O_{1-x}N_x)$. The urea/(Zn + Ga) molar ratios were chosen to be 3, 5, and 7. The Zn/Ga ratio varied between 49 and 6. The above solution combustion preparation procedure is similar to that of $ZnO_{1-x}N_x$ materials preparation.[4a]

2.2. Characterization Methods. Powder X-ray diffraction (XRD) data of $(Zn_{1-z}Ga_z)(O_{1-x}N_x)$ material was collected on a Rigaku X-ray diffractometer (DMAX IIIVC) equipped with a Ni-filtered Cu Kα radiation (λ = 1.542 Å) and graphite crystal monochromator. Selected samples of XRD data were collected on Philips X' Pert Pro diffractometer. The data were collected with a step size of 0.02° and a scan rate of 0.5°/min The observed interplanar *d* spacing was corrected with respect to Si. Rietveld refinement of the selected powder XRD profiles was carried out using the X'Pert Plus software.[4a] The standard deviation of the least-squares fit of an observed intensity profile was typically less than 0.002° 2θ. Surface area of the samples was estimated by N_2-adsorption/desorption isotherms, measured at −196 °C (NOVA 1200 Quanta Chrome equipment). Diffuse reflectance UV−vis measurements were carried out on a Shimadzu spectrophotometer (model UV-2550) with spectral-grade $BaSO_4$ as reference material. Raman spectra were recorded on a Ranishaw 2000 Raman microscope excited with 633 nm laser.[6]

X-ray photoelectron spectra (XPS) were recorded on VG Microtech Multilab ESCA 3000 spectrometer equipped with Al Kα or Mg Kα X-ray sources.[6] BE calibration was performed with Au($4f_{7/2}$) core level at 83.9 eV. Secondary ion mass spectrometry (SIMS) studies were carried out with a QMS-based instrument (Hiden Analytical). Bombardment was done with 5 keV oxygen and cesium ions. Primary ion current was 400 nA (oxygen beam) and 100 nA (cesium beam). The beam was rastered over an area of 1000 μm^2; however, the secondary ions were collected from the central 200 μm^2 area. Thermal analysis experiments were measured in Perkin-Elmer's Diamond TG/DTA at a rate of 10 °C/min in air or N_2 atmosphere.[6]

2.3. Catalytic Reactor. The reactor setup used for the nitrogen fixation to ammonia consists of mass flow controllers through which the reactant gases (N_2:H_2 = 1:3) pass at a controlled flow at a rate of 60 mL/min. The gases were mixed in the mixing chamber and fed to a series of traps for removing CO_2 (anhydrous KOH), moisture (fused $CaCl_2$ and molecular sieves), and O_2 (Cu-mesh maintained at a temperature of 300 °C). The mixture of gases was then allowed to pass through a quartz reactor loaded with the catalyst which was maintained at a temperature of 350 °C. The outgoing gases were then trapped in standardized H_2SO_4 (0.01 N) solution. The acid trap was designed in such a way that the gases were bubbled twice in two compartments before it is escaping to the atmosphere, ensuring the maximum trapping of NH_3 which is formed. Ammonia was estimated by the volumetric titration of the acid with NaOH (0.001) solution after the reaction. For rapid gas dissolution the trap acid solution was stirred on a magnetic stirrer, and the trap was placed inside a beaker with ice cold water. This ensures cooling of hot gases coming out of the reactor outlet and thus maximizes the solubility of the NH_3 in acid solution.

3. Results and Discussion

Figure 1 shows the X-ray diffraction (XRD) patterns of the $(Zn_{1-z}Ga_z)(O_{1-x}N_x)$ materials. Urea/(Zn + Ga) molar ratio and Ga atom % are given after UZ and G, respectively, in material codes, unless specified. Nitrogen incorporated ZnO (UZ7) shows typical ZnO features, and a small amount of zinc carbonate was observed on UZ7; it is due to effective combustion of urea that produces CO_2, as explained in our earlier report on $ZnO_{1-x}N_x$.[4] XRD results of $(Zn_{1-z}Ga_z)(O_{1-x}N_x)$ materials confirm the retention of the hexagonal Wurtzite phase ($P6_3mc$)[1] up to 12% Ga, above which there is a gradual formation of Ga_2O_3. All the peaks were indexed to ZnO, and no impurity phase was observed in the XRD patterns up to 12% Ga, which suggests that Ga^{3+} replaces Zn^{2+} in the ZnO lattice. No carbonate formation was observed in XRD as well as in photoemission results, indicating the suppression of carbonate formation in the presence of Ga. Positions of the major diffraction peaks were successively shifted to higher diffraction angles with increasing Ga%, indicating that the $(Zn_{1-z}Ga_z)(O_{1-x}N_x)$ materials are likely to be solid solutions of GaN and ZnO.[5,7] This peak shift is reasonable, as the size of Ga^{3+}

(6) (a) Vijayaraj, M.; Gopinath, C. S. *J. Catal.* **2006**, *243*, 376. (b) Joly, V. L. J.; Joy, P. A.; Date, S. K.; Gopinath, C. S. *J. Phys.: Cond. Matt.* **2001**, *13*, 649. (c) Waghmode, S. B.; Vetrivel, R.; Hegde, S. G.; Gopinath, C. S.; Sivasanker, S. *J. Phys. Chem. B* **2003**, *107*, 8517. (d) Gopinath, C. S.; Subramanian, S.; Prabhu, P. S.; Rao, M. S. R.; Subba Rao, G. V. *Physica C* **1993**, *218*, 117.

(7) (a) Maeda, K.; Teramura, K.; Lu, D.; Takata, T.; Saito, N.; Inoue, Y.; Domen, K. *Nature* **2006**, *440*, 295. (b) Maeda, K.; Teramura, K.; Takata, T.; Hara, M.; Saito, N.; Toda, K.; Inoue, Y.; Kobayashi, H.; Domen, K. *J. Phys. Chem. B* **2005**, *109*, 20504.

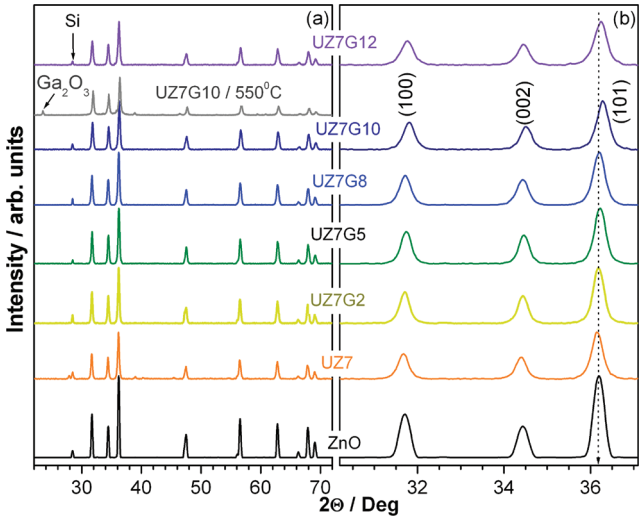

Figure 1. (a) Wide angle powder X-ray diffraction patterns of $(Zn_{1-z}Ga_z)(O_{1-x}N_x)$, prepared with urea/(Zn + Ga) = 7, $ZnO_{0.93}N_{0.07}$ (UZ7), and ZnO. (b) Main diffraction lines are shown in an expanded way for better clarity. The zinc carbonate feature was observed on UZ7 at 38.9°; however, no impurity features were observed on Ga and N codoped ZnO materials. Si was added with all the samples as an internal standard, and it appears at 28.45°.

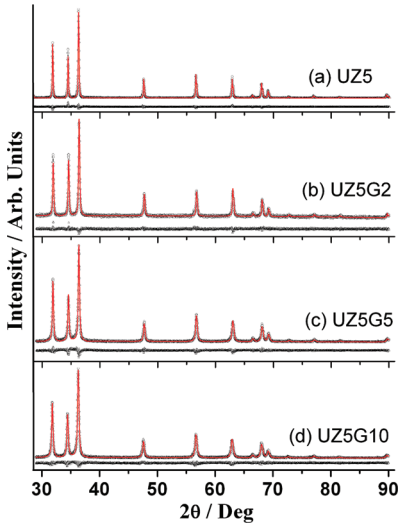

Figure 2. Rietveld refinement profiles of (a) UZ5, (b) UZ5G2, (c) UZ5G5, and (d) UZ5G10 $(Zn_{1-z}Ga_z)(O_{1-x}N_x)$ materials prepared by the solution combustion method. Experimental data points are given as open circles, and calculated intensity is given as red colored lines. The difference plot is given at the bottom.

(0.62 Å) is smaller than that of Zn^{2+} (0.72 Å). The same tendency was confirmed by Rietveld analysis. Rietveld refinement analysis of $ZnO_{1-x}N_x$[4] and Ga and N co-doped $(Zn_{1-z}Ga_z)(O_{1-x}N_x)$ materials is given in Figure 2. Similar analysis was carried out for UZ7G5 and UZ7G10 materials and is given in Supporting Information (Figure SI-1). An excellent agreement between the experimental and the fitted data indicated that the XRD pattern could be indexed satisfactorily to the Wurtzite structure with a space group of $P6_3mc$. Composition of UZ5-series materials with lattice parameters and surface area is given in Table 1. A linear decrease in *a* and *c* lattice parameters with increasing Ga% was observed. A systematic incorporation of Ga^{3+} ions in the Zn^{2+} site, the lattice

Table 1. Physicochemical Parameters of $(Zn_{1-z}Ga_z)(O_{1-x}N_x)$

material code and composition[a]	surface area (m^2/g)	*a* (Å)	*c* (Å)
UZ5G2—$Zn_{0.98}Ga_{0.02}O_{0.91}N_{0.09}$	5	3.2504(4)	5.2052(2)
UZ5G5—$Zn_{0.95}Ga_{0.05}O_{0.9}N_{0.1}$	9	3.2405(7)	5.1907(2)
UZ5G8—$Zn_{0.92}Ga_{0.08}O_{0.88}N_{0.115}$	12	3.2354(5)	5.1873(2)
UZ5G10—$Zn_{0.9}Ga_{0.1}O_{0.84}N_{0.15}$	17	3.2318(8)	5.1833(3)
UZ5G12—$Zn_{0.88}Ga_{0.12}O_{0.85}N_{0.15}$	18	3.2315(6)	5.1846(2)
UZ5G15—$Zn_{0.85}Ga_{0.15}O_{0.93}N_{0.08}$	20	3.2239(4)	5.1731(3)
UZ5—$ZnO_{0.914}N_{0.086}$	7	3.2421(5)	5.1924(2)
ZnO	60	3.250	5.205
GaN		3.188	5.183

[a] Urea/(Zn + Ga) = 5 and Ga atom % is given after G in the sample code. Material composition was determined from XRF and EDX.

parameters are expected to decrease, due to the smaller ionic radius of the former compared to the latter. Indeed, a decrease in the lattice parameter from *a* = 3.2504 Å (*c* = 5.2052 Å) to 3.2239 Å (5.1924 Å) was observed from 2% Ga to 15% Ga, respectively. This confirms that at least most of Ga^{3+} ions are incorporated in the zinc oxide lattice forming homogeneous $(Zn_{1-z}Ga_z)(O_{1-x}N_x)$ solid solutions. Incorporation of compensating N^{3-} and Ga^{3+} content offsets local lattice deformation and minimizes the lattice strain.[5] To a large extent, charge compensation was also taken care of by the above codoping. Further, this too allows the N-acceptor to exist in a stable anionic state.

Figure 3a depicts thermogravimetric analysis of $(Zn_{1-z}Ga_z)(O_{1-x}N_x)$ powders in air and nitrogen atmosphere. The initial weight loss up to 1% was observed below 200 °C is attributed to water loss. Weight loss continues up to another 1−2%, depending on the material composition, until 550 °C is due to some carbon removal and oxygen loss. No significant weight loss observed in nitrogen atmosphere, compared to the same material (UZ5G5) in air, supports the above conclusion. Nevertheless, a weight gain occurs above 600 °C in air atmosphere for all Ga-containing materials. The above weight gain is attributed to simultaneous N-loss and Ga_2O_3 formation. TGA in nitrogen atmosphere shows lower weight loss, and no weight gain above 700 °C confirms that the weight gain in air atmosphere is due to Ga_2O_3 formation. This is further confirmed from the XRD pattern of 800 °C calcined UZ7G10 (Figure 3b), displaying a mixture of Ga_2O_3 and ZnO. This indicates the N-atoms in the lattice were replaced progressively by oxygen above 600 °C to Ga_2O_3 and ZnO.

Figure 4 shows UV−visible absorption spectra of $(Zn_{1-z}Ga_z)(O_{1-x}N_x)$ materials along with standard ZnO and GaN for comparison purposes. ZnO and GaN shows absorption onset at 375 and 365 nm, respectively. A broad visible absorption band at 480 nm with low intensity is observed on UZ5 ($ZnO_{0.914}N_{0.086}$), apart from the typical absorption cutoff for ZnO at 375 nm. The energy difference between the above two features demonstrates the creation of a midgap (deep level acceptor) state in the band gap. Despite a high nitrogen content, no hole conductivity was observed and all $ZnO_{1-x}N_x$ ($x \leq 0.15$) materials exhibit insulating characteristics similar to that of ZnO.[4a] Indeed, the above observation supports the

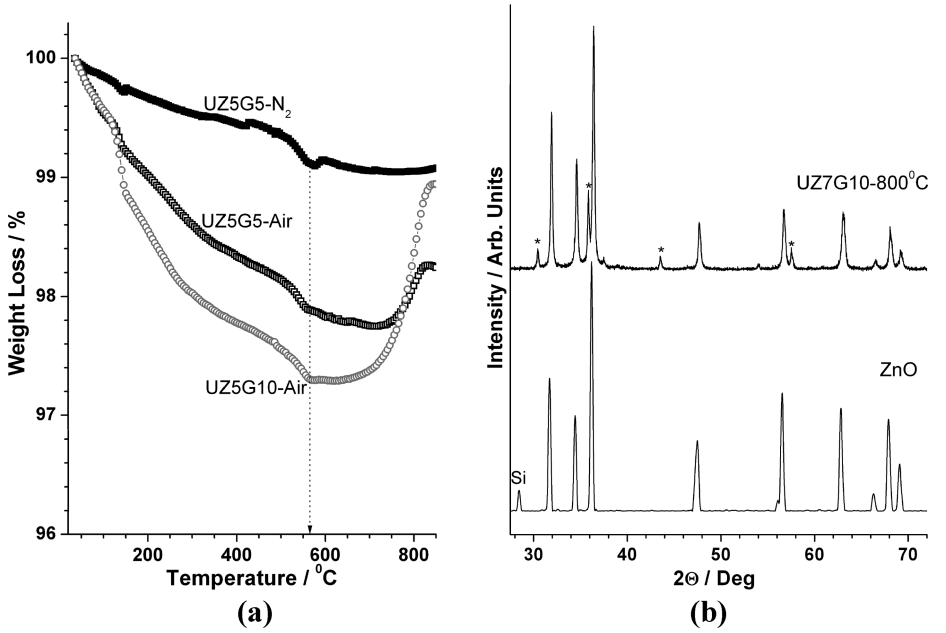

Figure 3. (a) Thermogravimetric analysis of $(Zn_{1-z}Ga_z)(O_{1-x}N_x)$ powders in air atmosphere and (b) XRD patterns of ZnO and UZ7G10 calcined at 800 °C for 6 h. Formation of Ga_2O_3 is evident from the weight gain at > 600 °C in TGA and from the additional peaks appear and marked with * on calcination.

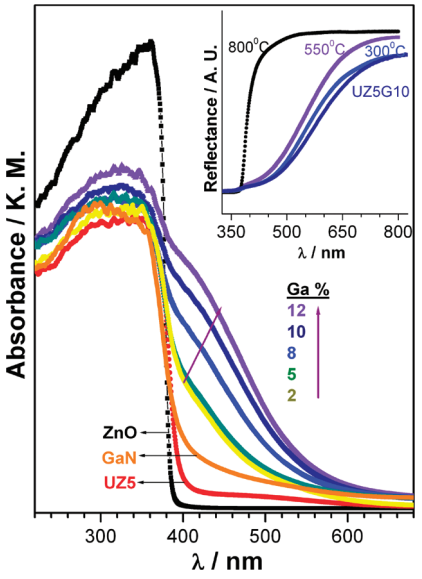

Figure 4. UV−visible absorption spectra of $(Zn_{1-z}Ga_z)(O_{1-x}N_x)$ materials, prepared with urea/(Zn + Ga) = 5, GaN, and ZnO. Inset shows the UV−vis reflectance spectra obtained from calcined UZ5G10 materials.

conclusion that the N 2p states are far removed from the top of the O 2p valence band and suggests the creation of N 2p derived midgap states in the forbidden gap of ZnO.[4a] No change in the conductivity of UZ5, compared to ZnO, underscores the generation of deep level acceptors. Interestingly, codoping of Ga and N displays an absorption onset around 550 nm and extends into the UV regime. Band maximum in the visible region shows a red shift from 410 to 450 nm for 2−12% Ga, respectively. A new band observed in the visible region shows an intensity comparable to that of the band in the UV regime, suggesting the large density of states in the new band at high Ga content. The above codoping helps to form shallow acceptor and donor levels and decreases the optical band gap to about 2.5 eV, depending on the composition of $(Zn_{1-z}Ga_z)(O_{1-x}N_x)$. A good overlap between N 2p (from nitride) and O 2p derived states at the valence band and 4s and 4p states from Ga and Zn at the conduction band is attributed to the above decrease in band gap. A physical mixture of ZnO and GaN does not show any absorption in the visible region, which underscores the true solid solution nature of $(Zn_{1-z}Ga_z)(O_{1-x}N_x)$.[7] Calcination of $(Zn_{1-z}Ga_z)(O_{1-x}N_x)$ (UZ5G10) in air at < 550 °C shows only minor changes in optical absorption characteristics (inset in Figure 4). However, calcination at > 550 °C leads to a fast decrease in the visible absorption band, and the 800 °C calcined material shows an optical absorption similar to that of ZnO . This is in good correspondence to weight gain at > 600 °C in TGA and Ga_2O_3 formation in XRD for the 800 °C calcined material. The above observations indicate that the visible light absorption is mostly due to nitride.

It is also to be mentioned here that interstitial zinc and oxygen vacancies are present in the $(Zn_{1-z}Ga_z)(O_{1-x}N_x)$ material, and it is mainly to compensate for the excess anionic charge from the significantly large nitrogen content and to maintain the charge neutrality of the entire lattice. Electron paramagnetic resonance studies (see Supporting Information, Figure SI-2) have been measured at room temperature, and representative results from UZ5, UZ5G5, and UZ5G10 are shown in Figure SI-2. This shows features that are due to Zn vacancies at $g = 2.00$, but relatively lower intensity for oxygen vacancies at lower field were observed.[4a] Three different oxygen vacancies observed on UZ5 changed to a broad feature for Ga-containing materials. A relatively higher (lower) zinc (oxygen) vacancy in Ga-containing materials is to be noted. No features due to nitric oxide (NO)-type species are observed, which suggests the absence of direct N−O linkages.

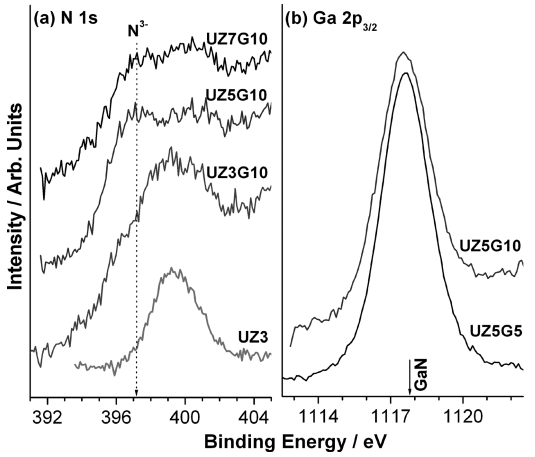

Figure 5. XPS spectra from (a) N 1s and (b) Ga $2p_{3/2}$ core levels of $(Zn_{1-z}Ga_z)(O_{1-x}N_x)$.

XPS of $(Zn_{1-z}Ga_z)(O_{1-x}N_x)$ was recorded and shown in Figure 5 for N 1s and Ga $2p_{3/2}$ core levels. The N 1s peak appears at a binding energy (BE) of 399.4 eV on UZ3 indicating the charge density on N is similar to that of NH_3 and primary amine compounds.[4,8] However, $(Zn_{1-z}Ga_z)(O_{1-x}N_x)$ shows an additional N 1s peak at 397 eV, and this feature is attributed to nitride (N^{3-}), along with the above peak. Indeed, XPS analysis of GaN shows the N 1s peak at 397 eV,[7,8] and confirms the presence of N^{3-}. XPS for Ga $2p_{3/2}$ core level appears at BE 1117.6 eV, indicating the Ga^{3+} state as in GaN. It is clear that the charge density of N in $ZnO_{1-x}N_x$ is as that of NH_3, but Ga and N codoping helps to form N^{3-} through GaN. As a result of the above, the optical absorption onset of $(Zn_{1-z}Ga_z)(O_{1-x}N_x)$ is shifted to higher wavelengths (Figure 4). It is likely that a strong mixing of 4s and 4p states of Zn and Ga near CB and O and N 2p states in the VB is responsible for the narrow band gap.[9]

Figure 6 shows XPS results obtained from Zn $2p_{3/2}$ and O 1s core levels of $(Zn_{1-z}Ga_z)(O_{1-x}N_x)$. A decrease in Zn $2p_{3/2}$ BE from 1021.7 eV on UZ5 to around 1021.4 eV upon Ga and N codoping in ZnO indicates an overall increase in electron density on Zn in the former.[4,8] Indeed, the ZnO BE appears at 1022 eV[4,8] and suggests that the electron density on Zn in $(Zn_{1-z}Ga_z)(O_{1-x}N_x)$ is significantly higher than that of ZnO. Further, a significant decrease in full width at half-maximum for $(Zn_{1-z}Ga_z)(O_{1-x}N_x)$ materials (2.2 eV) was observed compared to ZU5 (2.7 eV). The O 1s core level peak is broad for UZ5 at 531 eV compared to $(Zn_{1-z}Ga_z)(O_{1-x}N_x)$ at 530.4 eV indicating that at least two kinds of oxygen species were present on UZ5. Deconvolution demonstrates (not shown) that the peak at 530.5 eV is due to the ZnO crystal lattice oxygen, while the peak at about 532 eV is due to carbonate oxygen.[4a] The C 1s core level shows some carbonate features at 289 eV, and no other carbon was

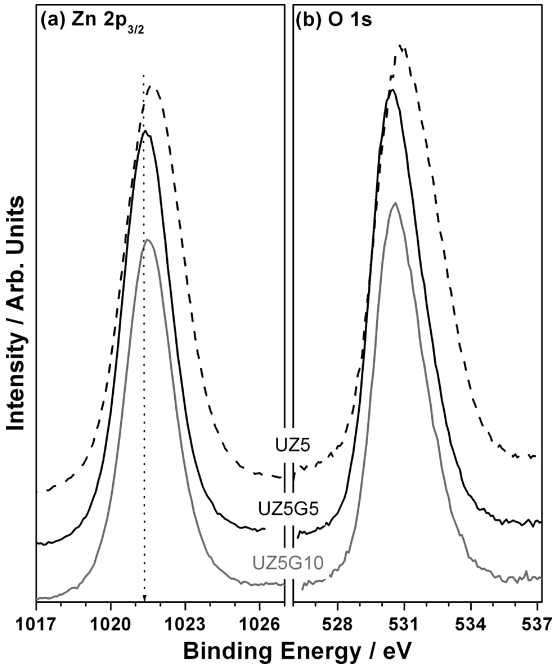

Figure 6. XPS core level spectra obtained from UZ5, UZ5G5, and UZ5G10 for (a) Zn $2p_{3/2}$ and (b) O 1s core levels.

observed. However, there is no carbonate observed in Ga-containing materials, and UZ5G5 and UZ5G10 show a narrow O 1s peak (fwhm = 2.5 eV) at 530.5 eV corresponding to that of ZnO. The above details from XPS suggest that the nature of Zn and O is relatively electron rich compared to its UZ5 counterpart; however, lower width also suggests a uniform distribution of GaN in ZnO.

Figure 7a shows the Raman spectra of UZ5, ZnO, and $(Zn_{1-z}Ga_z)(O_{1-x}N_x)$ materials. A sharp peak observed at 437 cm^{-1} is due to E_2(high) Raman active phonon mode of ZnO,[10] and its intensity decreases very significantly on $(Zn_{1-z}Ga_z)(O_{1-x}N_x)$. However, Raman active phonon modes of GaN[10] are also observed at 560, 579, and 730−740 cm^{-1} corresponding to E_1(TO) and E_2(high), A_1(LO), and E_1(LO), respectively. A broad peak observed at 582 cm^{-1} is attributed to the A_1(LO) and E_1(LO) mode of $ZnO_{1-x}N_x$.[4a] It is to be noted that this peak shows low (high) intensity for ZnO ($ZnO_{1-x}N_x$). Some of the above modes overlap around 575 cm^{-1}, and a broad feature observed for $z \leq 5\%$ in $(Zn_{1-z}Ga_z)$-$(O_{1-x}N_x)$ is due to heterogeneous near-neighbor environments. However, it becomes sharper at high z ($> 5\%$) values, hinting at a more homogeneous environment and supporting the solid solution nature of the materials. Two peaks at 510 and 642 cm^{-1} are due to the Zn−N related modes.[10] A sharp decrease in the intensity of E_2(high) (ZnO) at the expense of the Zn−N and Ga−N related

(8) (a) http://srdata.nist.gov/xps/ (accessed January 2009). (b) N 1s spectra were recorded with Mg K_α, to ensure that no contribution from Ga-$L_2M_{45}M_{45}$ Auger level (~392 eV with Al K_α) to the N 1s region.

(9) (a) Wei, S. H.; Zunger, A. *Phys. Rev. B* **1988**, *37*, 8958. (b) Ikarashi, K.; Sato, J.; Kobayashi, H.; Saito, N.; Nishiyama, H.; Inoue, Y. *J. Phys. Chem. B* **2002**, *106*, 9048.

(10) (a) Wang, D.; Seo, H. W.; Tin, C. C.; Bozack, M. J.; Williams, J. R.; Park, M.; Santhitsuksanoh, N.; Cheng, A.; Tzeng, Y. H. *J. Appl. Phy.* **2006**, *99*, 113509. (b) Haboeck, U.; Hoffmann, A.; Thomsen, C.; Zeuner, A.; Meyer, B. K. *Phys. Status Solidi B* **2005**, *242*, R21. (c) Hasuike, N.; Fukumura, H.; Harima, H.; Kisoda, K.; Matsui, H.; Saeki, H.; Tabata, H. *J. Phys.: Condens. Matter* **2004**, *16*, S5807. (d) Liu, H.-L.; Chen, C.-C.; Chia, C.-T.; Yeh, C.-C.; Chen, C.-H.; Yu, M.-Y.; Keller, S.; DenBaars, S. P. *Chem. Phys. Lett.* **2001**, *345*, 245.

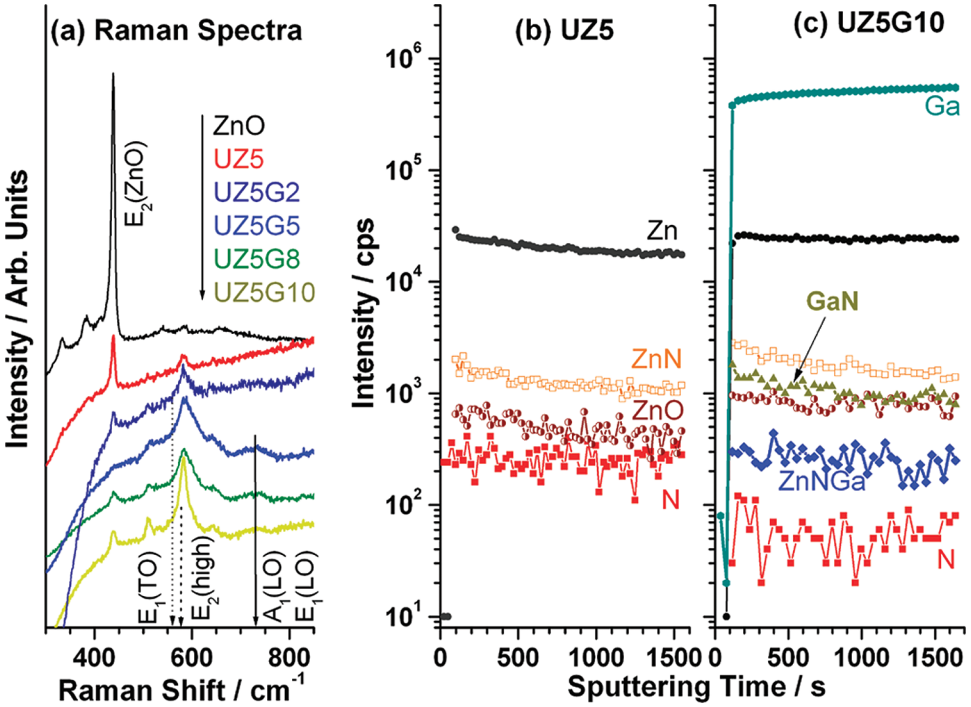

Figure 7. (a) Raman spectra from N 1s core levels of ZnO, UZ5, and $(Zn_{1-z}Ga_z)(O_{1-x}N_x)$. Secondary ion intensities of various species as a function of sputtering time are given for (b) UZ5 and (c) UZ5G10.

Raman active features suggests an increase in covalent character of the material.

Figure 7b,c shows the representative results obtained from the SIMS analysis of UZ5 and UZ5G10. Secondary ion intensities of different species as a function of sputtering time reflect the presence of the corresponding constituents as a function of depth. The presence of N (from N and ZnN) was observed on all the materials, apart from the expected species, such as Zn, ZnO, and Ga. Additionally, the direct observation of GaN from UZ5G10 underscores the solid solution of GaN in ZnO. Zn−N−Ga species suggests a direct interaction between N^{3-} to Zn also. Crucially, signal intensities remain constant at deeper levels from the surface, highlighting the solid solution nature and uniform distribution. This conclusion corroborates well with Raman and XPS results. That no GaO or NO species was observed suggests the efficacy of the combustion method to introduce N^{3-} in the ZnO lattice in a overall reductive atmosphere. It is to be noted that the intensity of ZnO is relatively lower compared to that of ZnN or GaN (Figure 7b,c), despite the fact that the volume content of ZnO (parent) is much higher than the doped species. This is attributed to the fact that the ionization efficiency of certain emitted species is dependent on local surface chemistry of the sample, known as "matrix effect" in SIMS.[11]

The presence of GaN in $(Zn_{1-z}Ga_z)(O_{1-x}N_x)$ and supported by physicochemical analysis underscores the importance of reaction atmosphere generated in the present experimental conditions. It is also to be noted that typical nitridation of oxides requires passing ammonia for several hours to a couple of days at high temperatures.[7] Nonetheless, formation of solid solution of GaN in ZnO hinted at the formation of high flux ammonia at high temperatures (~700 °C) under preparation condition. Indeed, gas-phase analysis of evolved gases shows predominantly ammonia along with some CO_2. However, a uniform distribution of small clusters of GaN in ZnO is unexpected, especially under the vigorous reaction conditions employed in the present work. Theoretical calculations reported by Schaefer et al.[12] predict small clusters of a size between 30 and 40 oligomers of GaN under similar conditions and are in good agreement with our experimental results.

Table 2. Ammonia Synthesis Activity on $(Zn_{1-z}Ga_z)(O_{1-x}N_x)$

catalyst	time on stream (h)	amount of ammonia (mmol h^{-1} g^{-1})
UZ5G10	1	0.44
	2	0.48
	3	0.42
UZ7G10	1	1.51
	2	0.74
	3	0.24

$(Zn_{1-z}Ga_z)(O_{1-x}N_x)$ materials were explored for heterogeneous catalysis applications. Although these materials display high catalytic activity for conventional reactions like 2-butanol to 2-butanone selectively at 400 °C, due to the presence of a significantly large amount of nitride in the above material, it has been explored for ammonia synthesis. Bimetallic nitrides are known to be active for NH_3 production at high pressure.[13] The

(11) Chakraborty, P. Ion beam analysis of surfaces and interfaces in condensed matter systems; Chakraborty, P., Ed.; Nova Science Publishers: New York, 2002.

(12) Timoshkin, A. Y.; Schaefer, H. F.III *J. Phys. Chem. A* **2008**, *112*, 13180 and references therin .

(13) Jacobsen, C. J. H. *Chem. Commun.* **2000**, 1057 and references therein .

presence of GaN and Ga−N−Zn species on $(Zn_{1-z}Ga_z)$-$(O_{1-x}N_x)$ lead us to explore N_2 fixation through NH_3 formation with the $N_2 + 3H_2$ mixture at 350 °C at ambient pressure, especially in view of the drastic changes in electronic structure of $(Zn_{1-z}Ga_z)(O_{1-x}N_x)$, such as decrease in band gap to 2.5 eV, direct Zn−N and Ga−N bonds, solid solution nature, and so forth compared to ZnO. Representative reaction results are given in Table 2.

Nitrogen doped ZnO (UZ5 and UZ7), but without Ga, does not show any activity toward ammonia formation. UZ5G10 shows almost the same activity (0.44 mmol/(h g)) for the first three hours and then decreases rapidly. The maximum NH_3 formation activity of 1.51 mmol/(h g) was observed on UZ7G10 for first hour, and then it decreases with increasing time on stream. No significant ammonia production was observed above 3 h. UZ7G10 catalytic activity is comparable to that of Co_3Mo_3N;[13] however, the activity is an order of magnitude less than that of commercial or Cs-promoted Co_3Mo_3N catalysts (15 −30 mmol/(h g)). It is to be noted that the above activity reported with commercial or Cs-promoted bimetallic catalysts was measured at 400 °C and 100 bar and with electronic promoters.[13] It is to be noted that the present reaction was at ambient pressure, 350 °C, without any promoter, and the nitride content is far less than that of bimetallic nitrides.[13] This underscores the potential nature of $(Zn_{1-z}Ga_z)(O_{1-x}N_x)$ toward NH_3 synthesis and other catalytic reactions. The spent catalyst materials were analyzed for nitrogen content, and they show the same characteristics as those of freshly prepared catalysts, including the color. This underscores that the nitrogen in the solid solution is retained after reaction. No volatalization of Zn or Ga was also observed. Further studies are essential to confirm the catalytic activity as well as to explore the reasons behind this unusual activity. More studies are in progress to maximize the catalytic activity and to understand the deactivation mechanism.

4. Conclusions

Solid solution of GaN in ZnO $\{(Zn_{1-z}Ga_z)(O_{1-x}N_x)$ (x and $z = 0-0.15$)$\}$ has been prepared by the solution combustion method. XRD studies confirm the presence of Wurtzite phase, and the electronic spectra show visible light absorption and an optical band gap decreased to 2.5 eV compared to 3.4 eV with ZnO. Raman spectroscopy, XPS, and SIMS results suggest the presence of Zn−N and Ga−N bonds. The above results suggest the N 2p states from nitride occupy the states just above the O 2p VB and reduce the band gap. Catalytic activity toward N_2 fixation was observed at atmospheric pressure at 350 °C on $(Zn_{1-z}Ga_z)(O_{1-x}N_x)$, indicating its potential as a catalyst. Further studies are in progress.

Acknowledgment. CSG thank Dr. S. Sivaram for constant encouragement. Dr. Devendra S. Bhange's help in Rietveld analysis is acknowledged. MM, BS, CMN and CMJ thank CSIR, New Delhi for research fellowship.

Supporting Information Available: Figures showing Rietveld refinement data for UZ7G5 and UZ7G10 (Figure SI-1) and EPR spectra for UZ5, UZ5G5 and UZ5G10 (Figure SI-2) (PDF). This material is available free of charge via the Internet at http://pubs.acs.org.